Available online at www.sciencedirect.com
SCIENCE DIRECT®
International Journal of Thermal Sciences 44 (2005) 1090–1097
International Journal of Thermal Sciences
www.elsevier.com/locate/ijts

Optimal design and measurement of the effective thermal conductivity of a powder using a crenel heating excitation

Fethi Albouchi [a,*], Mourad Fetoui [a], Fabrice Rigollet [b], Mohamed Sassi [a], Sassi Ben Nasrallah [a]

[a] *Ecole Nationale d'Ingénieurs de Monastir, Laboratoire d'Etudes des Systèmes Thermiques et Energétiques, Avenue Ibn Eljazzar, 5019 Monastir, Tunisia*
[b] *Institut Universitaire des Systèmes Thermiques Industriels, UMR CNRS 6595, Ecole Polytechnique Universitaire de Marseille (Departament Mécanique Energétique), Technopôle de Château Gombert, 5 rue Enrico Fermi, 13453 Marseille cedex 13, France*

Received 11 February 2004; received in revised form 4 March 2005; accepted 13 April 2005
Available online 31 May 2005

Abstract

This paper presents an experimental optimal design of a photothermal radiometry method using a crenel heating excitation. This method is used for the determination of the effective thermal conductivity of a powder in imperfect contact with a coating, and in presence of convective heat losses. The parameter identification is performed by the minimization of the ordinary least squares objective function comparing the measured temperatures to the response of a direct model function of thermophysical parameters. The used iterative algorithm is based on the Gauss–Newton method.

Keywords: Two-layered materials; Thermal contact resistance; Effective thermal conductivity; Identification; Gauss–Newton; Crenel heating excitation

1. Introduction

Granular media are frequently encountered in different fields of science and industry. These materials often behave differently from ordinary single phase systems. Their thermophysical properties are of interest in the analysis, design and optimization of industrial processes and in the understanding of natural phenomena [1–5]. The majority of common methods used to characterize these systems are based on an effective medium description, which gives effective properties. These methods use many heating techniques. One of these techniques is the crenel heating excitation, which differs from others by using a constant source of light instead of a pulse. This method can be viewed as an extension of the well-known flash and the step-heating methods [6–8]. Its advantage is the relatively low intensity of the imposed heat flux.

The objective of this work is to study the feasibility of a photothermal crenel technique used for the characterization of effective thermophysical properties of a powder. The principal difficulties lie primarily in the porous structure of these materials: a significant contrast of conductivity exists between the solid and the fluid. For this reason, we consider the powder as an homogeneous medium, and we measure its effective properties. In this article we present the theoretical and the experimental study concerning the determination of the effective thermal conductivity of a powder. In the theoretical study, we are interested on the reduction of the thermal model and on the optimal design of the experiment. This optimal conception is analysed on a two layered sample with a known substrate volumetric capacity.

The powder is placed in a Teflon cell closed by a copper coating layer. The medium is modelled as a bi-layer composite. In these structures, the thermal contact resistance between the grains and copper affects heat transfer from one layer to the other [9–17]. Its value depends on the thermophysical properties and on the contact pressure.

In this paper, the thermal properties are identified by the minimization of the ordinary least squares (OLS) function that compares the measured temperature on the rear face of

* Corresponding author. Tel.: +216 98 627 180; fax: +216 73 500 514.
E-mail addresses: albouchif@yahoo.fr (F. Albouchi), mfetoui@yahoo.fr (M. Fetoui), fabrice.rigollet@polytech.univ-mrs.fr (F. Rigollet), mohamed.sassi@enim.rnu.tn (M. Sassi), ssbnsrl@ati.tn (S. Ben Nasrallah).

1290-0729/$ – see front matter
doi:10.1016/j.ijthermalsci.2005.04.003

Nomenclature

a_i	layer thermal diffusivity ..... $m^2 \cdot s^{-1}$	$\mathbf{T}_m$	experimental temperature ..... K
C_p	heat capacity ..... $J \cdot kg^{-1} \cdot K^{-1}$	z	space coordinate ..... m
e_i	layer thickness ..... m	$\mathbf{Z}_{ij}$	reduced sensitivity coefficient ..... K
h	heat transfer coefficient ..... $W \cdot m^{-2} \cdot K^{-1}$	*Greek symbols*	
$\mathbf{J}$	reduced Hessian matrix		
k_i	layer thermal conductivity ..... $W \cdot m^{-1} \cdot K^{-1}$	ρ	density ..... $kg \cdot m^{-3}$
p	Laplace parameter ..... s^{-1}	σ	standard deviation
$\mathbf{R}$	covariance matrix of the relative uncertainty on the estimated parameters	θ_f	Laplace temperature on the front face of the first layer ..... K·s
R_c	thermal contact resistance ..... $W^{-1} \cdot K \cdot m^2$	θ_r	Laplace temperature on the rear face of the second layer ..... K·s
S	surface ..... m^2	$\boldsymbol{\beta}_r$	parameter vector of the reduced model
t	time ..... s	ψ	density of heat flux ..... $W \cdot m^{-2}$
t_c	heating time ..... s	ξ	crenel excitation ..... $W \cdot m^{-2}$
$\mathbf{T}_{\text{cren}}$	calculated temperature ..... K		

the bi-layer during the crenel-heating experiment to the response of the theoretical model.

In the first part of the paper, we present the model, built with the thermal quadrupoles formalism, and the sensitivity analysis. Then, in the second part, we present the minimization method and the used tools to optimally design the experiment. Finally, we present and discuss the numerical and the experimental results for a glass powder.

2. Thermal model

2.1. General model

The model assumes one-dimensional heat flow through a two-layer sample constituted by two materials of thickness e_1 and e_2. Their interface is characterized by an imperfect contact (thermal contact resistance R_c). The thermal properties and densities of both layers are assumed to be uniform and constant. The convective and radiative heat transfer on the two faces with the uniform environment are expressed by two heat transfer coefficients h_1 and h_2. The lateral heat exchanges are neglected. At time $t = 0$, we assume that the system is in thermal equilibrium, i.e. $T(t = 0) = 0$. The front face of the sample is uniformly subjected to a constant crenel heat flux $\xi(t)$ (Fig. 1):

$$\xi(t) = \begin{Bmatrix} \psi & 0 \leqslant t \leqslant t_c \\ 0 & t \geqslant t_c \end{Bmatrix} \tag{1}$$

where t_c is the duration of the applied heating.

The transient temperature distribution in the sample can be obtained by solving the one dimensional heat conduction equation for each layer:

$$k_i \frac{\partial^2 T_i(z,t)}{\partial z^2} = \rho_i C_i \frac{\partial T_i(z,t)}{\partial t}, \quad i = 1, 2 \tag{2}$$

where T_i is the temperature of layer i.

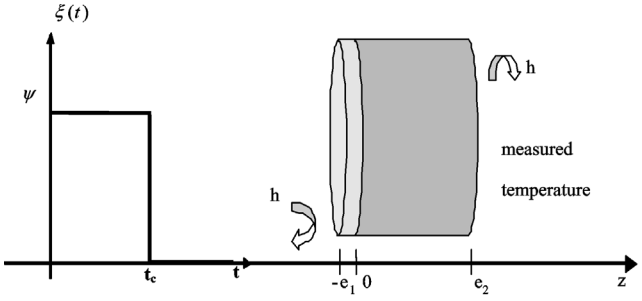

Fig. 1. Principle of the crenel transient method.

Coupled to arbitrary initial and boundary conditions:

$$T_i = 0 \quad \text{at } t = 0 \tag{3}$$

$$-k_1 \frac{\partial T_1(-e_1,t)}{\partial z} = \xi(t) - h_1 T_1(-e_1,t) \quad \text{at } z = -e_1 \tag{4}$$

$$-k_1 \frac{\partial T_1(0,t)}{\partial z} = \frac{1}{R_c}\big(T_1(0,t) - T_2(0,t)\big) \quad \text{at } z = 0 \tag{5}$$

$$k_1 \frac{\partial T_1(0,t)}{\partial z} = k_2 \frac{\partial T_2(0,t)}{\partial z} \quad \text{at } z = 0 \tag{6}$$

$$k_2 \frac{\partial T_2(e_2,t)}{\partial z} = -h_2 T_2(e_2,t) \quad \text{at } z = e_2 \tag{7}$$

To solve this system, we have used the thermal quadrupole method [18]. The entire system can be described in Laplace space as

$$\begin{bmatrix} \theta_f \\ \frac{\psi(1-\exp(-pt_c))}{p} \end{bmatrix} = \begin{bmatrix} 1 & 0 \\ h_1 S & 1 \end{bmatrix} \begin{bmatrix} A_1 & B_1 \\ C_1 & D_1 \end{bmatrix} \begin{bmatrix} 1 & R_c \\ 0 & 1 \end{bmatrix} \times \begin{bmatrix} A_2 & B_2 \\ C_2 & D_2 \end{bmatrix} \begin{bmatrix} 1 & 0 \\ h_2 S & 1 \end{bmatrix} \begin{bmatrix} \theta_r \\ 0 \end{bmatrix} = \begin{bmatrix} A & B \\ C & D \end{bmatrix} \begin{bmatrix} \theta_r \\ 0 \end{bmatrix} \tag{8}$$

Here θ_f and θ_r are the Laplace transforms of the sample front and rear face temperatures, respectively. The coefficients A_i, B_i, C_i and D_i depend on the Laplace parameter p,

on the thickness e_i of the layer i and on the thermophysical properties of the material. They are given by

$$A_i = D_i = \cosh(\alpha_i e_i)$$
$$C_i = k_i \alpha_i S \sinh(\alpha_i e_i)$$
$$B_i = \frac{1}{k_i \alpha_i S} \sinh(\alpha_i e_i)$$
$$\alpha_i = \sqrt{\frac{p}{a_i}}$$

The Laplace transform of the rear face temperature can be written as

$$\theta_r(p) = \frac{\psi(1 - \exp(-pt_c))}{pC} \tag{9}$$

with dimensional parameters, the rear face temperature can be expressed as

$$\theta_r(p) = f(p, t_c, a_1, k_1, e_1, a_2, k_2, e_2, h_1, h_2, R_c, \psi) \tag{10}$$

The temperature in the usual space domain $T_{\text{cren}}(t)$ is obtained by the inverse transform of $\theta_r(p)$ using the numerical algorithm proposed by Gaver–Stehfest [18]: This solution will represent the general model.

2.2. Reparametrization and reduction of the model

Owing to the large number of parameters encountered in the general model, the study is presented in dimensionless space with dimensionless parameters. Two approximations have been used. The first is to take the same heat transfer coefficient on the two sample faces ($h_1 = h_2 = h$) seeing that we work at ambient temperature. The second approximation is to consider that the first layer is purely capacitive. In this case the Laplace transform of the rear face temperature for a crenel heating excitation is given by[1]

$$\theta_{\text{cren,red}} = \frac{\beta_{r3}(1-\exp(-s_1^2 t_c^*))}{\beta_{r1}^2 s_1^4 [\delta(s_1,\beta_{r4},\beta_{r5}) + \phi(s_1,\beta_{r2},\beta_{r4},\beta_{r5}) + \varphi(s_1,\beta_{r3},\beta_{r5})]} \tag{11}$$

where

$$\delta(s_1, \beta_{r4}, \beta_{r5}) = \beta_{r4} \operatorname{ch}(s_1) + \left(1 + \beta_{r4}\beta_{r5} s_1^2\right) \frac{1}{s_1} \operatorname{sh}(s_1) \tag{12a}$$

$$\phi(s_1, \beta_{r2}, \beta_{r4}, \beta_{r5}) = \beta_{r2} \left[\left(\frac{2}{s_1^2} + \beta_{r4}.\beta_{r5} \right) \operatorname{ch}(s_1) + \left(\frac{\beta_{r5}}{s_1} + \frac{\beta_{r4}}{s_1} \right) \operatorname{sh}(s_1) \right] \tag{12b}$$

$$\varphi(s_1, \beta_{r3}, \beta_{r5}) = \beta_{r2}^2 \left[\frac{1}{s_1^3} \operatorname{sh}(s_1) + \frac{\beta_{r5}}{s_1^2} \operatorname{ch}(s_1) \right] \tag{12c}$$

The dimensionless parameters are defined by

$$s_1 = \sqrt{\frac{p}{\beta_{r1}}}, \qquad \beta_{r1} = \frac{a_2}{e_2^2}, \qquad t_c^* = \beta_{r1} t_c$$
$$\beta_{r2} = \frac{h e_2}{k_2}, \qquad \beta_{r3} = \frac{\psi}{\rho_2 C_{p2} e_2}$$
$$\beta_{r4} = \frac{\rho_1 C_{p1} e_1}{\rho_2 C_{p2} e_2}, \qquad \beta_{r5} = \frac{R_c . k_2}{e_2} \tag{13}$$

The calculated variations with time of the temperature $T_{\text{cren,red}}(t)$ can be calculated using the Stehfest inversion of $\theta_{\text{cren,red}}(p)$. This solution will represent the reduced model.

3. Sensitivity coefficients and optimal experiment design

The sensitivity coefficients are defined as the first derivatives of the measured variable with respect to the parameters of the model. Their reduced form shows the variation ∂T_{cren} of the model induced by a relative variation $\frac{\partial \beta_j}{\beta_j}$ of the parameter:

$$Z_{ij}(t) = \beta_j X_{ij}(t, \boldsymbol{\beta}) = \beta_j \frac{\partial T_{\text{cren}}(t, \boldsymbol{\beta})}{\partial \beta_j} \quad j = 1, 2, \ldots \tag{14}$$

In general, these reduced sensitivity coefficients must be large and uncorrelated with each other [19]. The covariance matrix of the relative uncertainty on the estimated parameters $\mathbf{R}$ is evaluated using the reduced Hessian matrix $\mathbf{J} = \mathbf{Z}^t\mathbf{Z}$, where $\mathbf{Z}$ is the $(n \times m)$ reduced sensitivity coefficients matrix. This covariance matrix is defined by the following expression:

$$\mathbf{R} = \mathbf{J}^{-1}\sigma^2 \tag{15}$$

where σ^2 is the variance of the measurements noise and $R_{ij} = \frac{\operatorname{cov}(\hat{\beta}_{ri}, \hat{\beta}_{rj})}{\beta_{ri}\beta_{rj}}$.

If we supposed the following conditions: we have the response over a dimensionless duration $t_n^* = \beta_{r1} t$ from $t_1^* = 0$, on a sufficiently large number n of measurements to assimilate the following sums (which constitute the components of $\mathbf{J}$) to the integrals:

$$J_{pq} = \sum_{i=1}^{n} Z_p(t_i^*) Z_q(t_i^*) \cong \frac{1}{\Delta t^*} I_{pq}(t_n^*) = \frac{n}{t_n^*} I_{pq}(t_n^*) \tag{16}$$

where $I_{pq}(t_n^*) = \int_0^{t_n^*} Z_p(t^*) Z_q(t^*)\, \mathrm{d}t^*$.

Under these conditions, we show that the reduced Hessian determinant varies with the measurements number in the following way:

$$\Delta\mathbf{J} = \det(\mathbf{J}) = n^m f_n(t_n^*) = \frac{1}{\Delta t^{*m}} f_t(t_n^*) \tag{17}$$

where m is the number of unknown parameters and $f_n(t_n^*) = \frac{f_t(t_n^*)}{(t_n^* - t_1^*)^m}$.

According to whether we fix, for each considered duration t_n^*, the time step Δt^* or the number of measurement n, the functions $f_n(t_n^*)$ and $f_t(t_n^*)$ are combinations of the various integrals of the type (16), calculated numerically. The relations (17) reveal two approaches to choose the optimal

[1] The new expression (11) is exact, but, in practice, we have used the superposition of the two step heating answers shifted in time, and having the same levels (one is positive and the second is negative).

duration of the experiment $(t_n^*)_{\text{opt}}$, corresponding to two different experimental constraints. A first user can desire to carry out a fixed acquisition number of measurements between 0 and t_n^* (for reasons of limited size of storage for example), he will have, from the first equality of (17), to maximize $f_n(t_n^*)$. A second user may have, on the other hand, a lower limit in the size of the acquisition time step Δt^* which he can put in use (band-width of the acquisition system). He will then have, from the second equality of (17), to choose the smallest Δt^* possible and to maximize $f_t(t_n^*)$ for maximizing $\Delta \mathbf{J}$.

A second criterion can be used for determining the optimal experiment duration. This criterion consist on minimizing the sums of squares, given by the diagonal of the covariance matrix $(\sigma^2_{\beta_{ri}}/\beta^2_{ri})$. This is an individual criteria, used when not all the parameters are of interest. It gives as many useful experiment durations as number of parameters.This later differs from the D-optimal criterion, which minimizes the volume of the confidence region, so it gives the optimal duration allowing the estimation of all unknown parameters.

4. Parameter identification method

The unknown thermal parameters are identified as the solution of the minimization of the gap between the measured temperature and the calculated temperature of the direct problem. This gap minimization is carried out by minimizing the least squares, given by

$$C(\boldsymbol{\beta}_r) = \sum_{i=1}^{n} \left(\mathbf{T}_{e_i} - \mathbf{T}_{\text{creni}}(\boldsymbol{\beta}_r)\right)^2 \tag{18}$$

where, $\mathbf{T}_e$ is a vector containing the measured temperatures, $\mathbf{T}_{\text{cren}}$ is a vector containing the calculated temperatures, and $\boldsymbol{\beta}_r$ is the parameter vector with m the number of estimated parameters and n the number of measurements.

In vectorial form, the solution vector $\boldsymbol{\beta}_{r,n+1}$ at the iteration $n+1$ can be written as

$$\boldsymbol{\beta}_{r,n+1} = \boldsymbol{\beta}_{r,n} + \left[\mathbf{X}(\boldsymbol{\beta}_{r,n})^t \mathbf{X}(\boldsymbol{\beta}_{r,n})\right]^{-1} \mathbf{X}(\boldsymbol{\beta}_{r,n})^t \times \left(\mathbf{T}_e - \mathbf{T}_{\mathbf{cren}}(\boldsymbol{\beta}_{r,n})\right) \tag{19}$$

5. Numerical results

5.1. Validity of the model

The methodology presented above is here applied to a Copper/PVC bi-layer system. The following thermophysical properties were assumed: for copper: $a_1 = 1.15 \times 10^{-4}$ m^2·s^{-1}, $C_{p1} = 384.9$ J·kg^{-1}·K^{-1} and $\rho_1 = 8940$ kg·m^{-3} and for PVC $a_2 = 1.14 \times 10^{-7}$ m^2·s^{-1}, $C_{p2} = 900$ J·kg^{-1}·K^{-1} and $\rho_2 = 1390$ kg·m^{-3}. The other parameters are taken to be: $e_1 = 0.6$ mm, $e_2 = 5$ mm, $R_c = 5 \times 10^{-4}$ m^2·K·W^{-1}, $h_1 = h_2 = 10$ W·m^{-2}·K^{-1} and $\psi = 10^5$ W·m^{-2}.

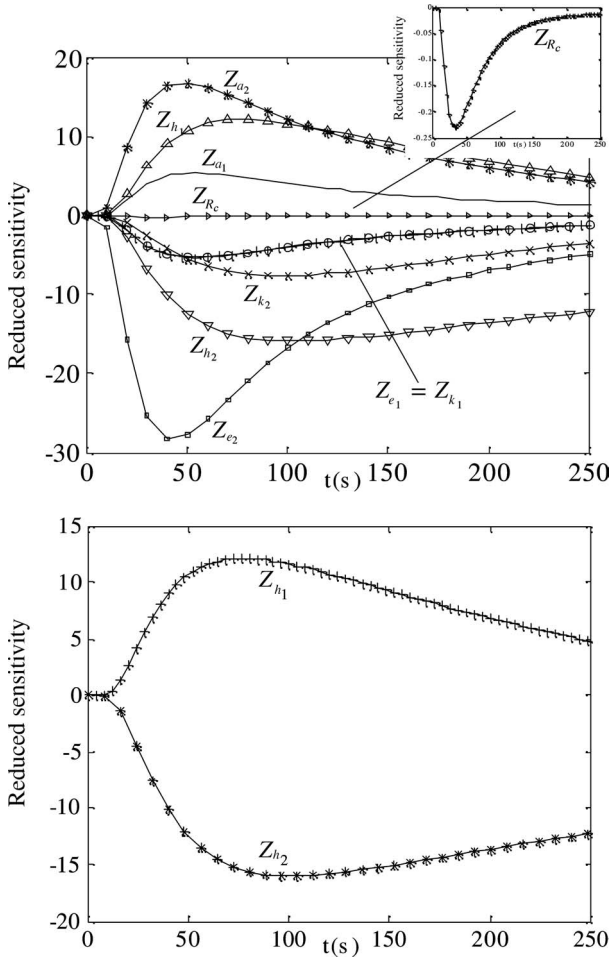

Fig. 2. Sensitivities of the general model.

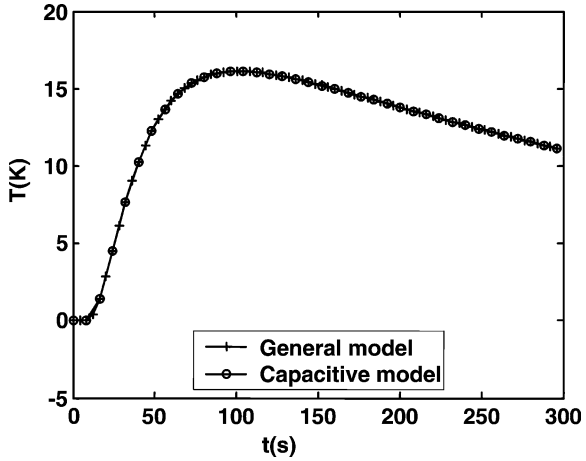

Fig. 3. Comparison between capacitive and general model.

In order to verify the approximations taken into account in the model reduction, we represent on Fig. 2, the sensitivity coefficients of the general model parameters. We remark that

Z_{h_1} and Z_{h_2} have the same shape and the same influence on the model. These two parameters are correlated, for this reason; we have chosen the same heat transfer coefficient on the two sample faces.

For the second approximation of capacitive layer, we present on Fig. 3 a comparison between the general and the capacitive model. We remark that the two models responses are identical. So our approximation is valuable.

5.2. Sensitivity analysis and optimal design

Fig. 4 presents the reduced sensitivity coefficients of the reduced model parameters versus time for two values of the thermal contact resistance ($R_c = 5 \times 10^{-3}$ and $R_c = 5 \times 10^{-4}$ m^2·K·W^{-1}). It can be seen that the curves $Z_{\beta_{r1}}$, $Z_{\beta_{r2}}$, $Z_{\beta_{r3}}$ and $Z_{\beta_{r5}}$ do not have the same form, and their maxima are reached at different times. These observations verify that these four sensitivity coefficients are uncorrelated, which is a desirable condition for parameter estimation. On the other hand, the curves $Z_{\beta_{r4}}$ and $Z_{\beta_{r5}}$ have the same shape and their maxima are almost reached at the same time. Therefore, these two sensitivity coefficients are correlated, and as a consequence, the parameters β_{r4} and β_{r5} cannot be identified simultaneously.

Given that the volumetric thermal capacity can be easily measured by a calorimetric experiment, we can fix the value of $\rho_2 C_{p2}$, so the parameter β_{r4} is considered to be known. At this stage, the reduced model depends only on four parameters.

For $R_c = 5 \times 10^{-4}$ m^2·K·W^{-1}, it can be seen that the reduced sensitivity of β_{r5} is very weak (almost null). So this parameter cannot be easily estimated.

For the experiment design, we present the first approach (n fixed). The curves $\sqrt[m]{f_n(t_n^*)}$ are plotted on Figs. 5 and 6 for two values of the Biot number, $\beta_{r2} = 0.1$ and $\beta_{r2} = 1$ respectively and for different heating time t_h^*. The heat flux is considered to be constant between times 0 and t_h^*. The constraints of a fixed large number of measurements and a same maximum temperature rise are used [20,21]. It is observed that the curves $\sqrt[m]{f_n(t_n^*)}$ pass through a maximum, which varies with the heating time t_h^* and the experiment duration t_n^*. This means that there are two optimal times in this experiment: the heating and the experiment duration.

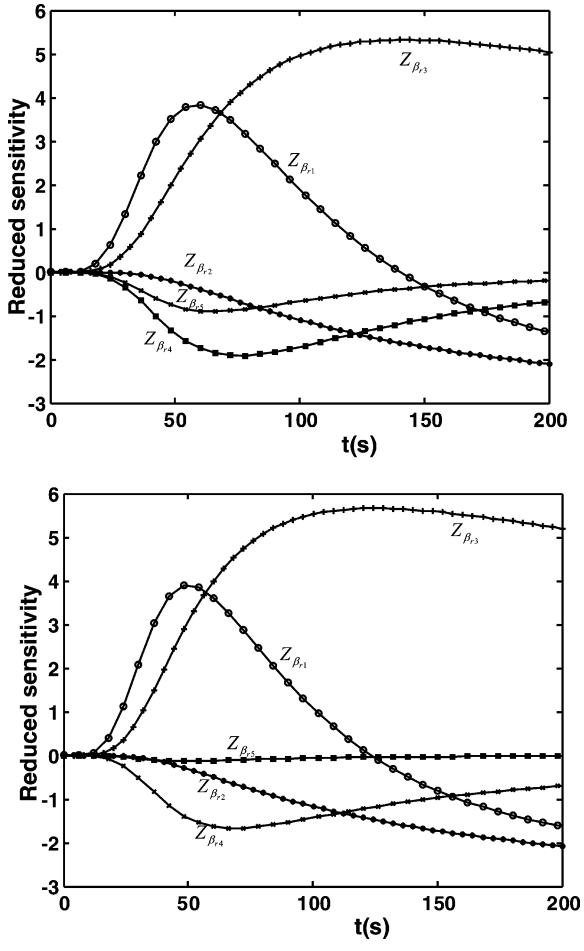

Fig. 4. Sensitivities of the reduced model for $R_c = 5 \times 10^{-3}$ and $R_c = 5 \times 10^{-4}$ W^{-1}·m^2·K.

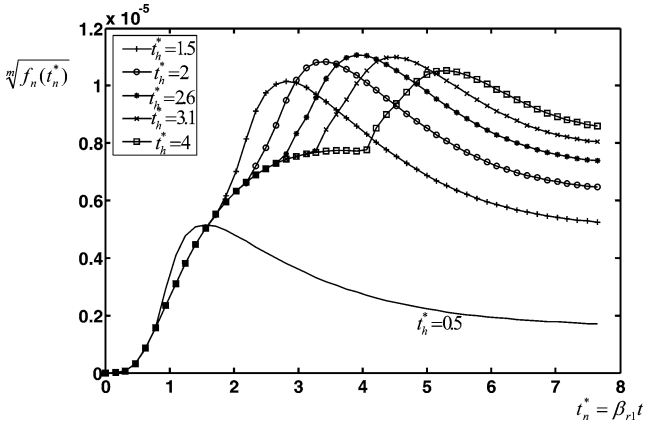

Fig. 5. $\sqrt[m]{f_n(t_n^*)}$ as function of the heating time and the experiment duration for $\beta_{r2} = 0.1$.

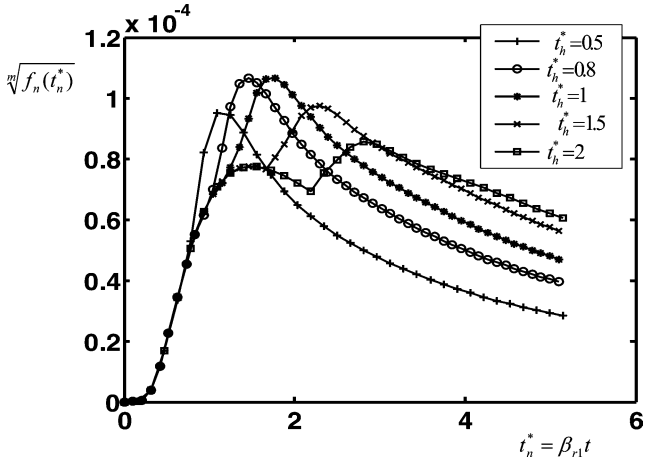

Fig. 6. $\sqrt[m]{f_n(t_n^*)}$ as function of the heating time and the experiment duration for $\beta_{r2} = 1$.

With n fixed, the optimal experiment duration $(t_n^*)_{\text{opt}}$ for estimation of the parameters is that for which $\sqrt[m]{f_n(t_n^*)}$ is maximum. It is an interesting criterion since it means that from this pointing time, the longer the experiment lasts, the less beneficial it is in terms of the parameter estimation precision.

We thus record on Figs. 5 and 6 the heating and the experiment durations for which $\sqrt[m]{f_n(t_n^*)}$ is maximum for the two values of the Biot number ($\beta_{r2} = 0.1$ and $\beta_{r2} = 1$). We obtain dimensionless durations of $(t_h^*)_{\text{opt}} = 2.6$ and $(t_n^*)_{\text{opt}} = 3.8$ for a weak exchange ($\beta_{r2} = 0.1$, Fig. 5), and $(t_h^*)_{\text{opt}} = 1$ and $(t_n^*)_{\text{opt}} = 1.8$ for a strong exchange ($\beta_{r2} = 1$, Fig. 6).

6. Experimental setup

The experimental device is schematically shown in Fig. 7. It includes a heat source, a sample, an infrared camera and a Hewlett Packard (HP)-based data acquisition system. The investigated sample (Fig. 8) is composed of a Teflon cell of thickness $e_2 = 5$ mm coated with a thin copper layer at the front face. This cell is filled with a glass powder, where the characteristics of which are presented on Table 1. The weight of the powder is 8.06 g and its porosity is $\varepsilon = 0.32$. The cell is horizontally maintained on a holder and it is heated below by a halogen lamp, which provides a uniform heat flux of power 150 W, with a finite duration. A mirror covered by a layer of gold reflect the flux emitted by the surface of the powder towards an infrared camera (AGEMA) working in the short wave range (3–5 μm) and cooled by a liquid nitrogen. This infrared camera is connected to an acquisition system allowing the storage and the visualization of the images. These infrared pictures are constituted of 100 lines and 256 columns and stored in real time in the monitor with a speed of 25 pictures per second. The camera does not give directly absolute temperatures but numerical levels proportional to the luminance of the sample. To access the absolute temperatures, some parameters must be known such as the emissivity of the powder and the standard constants of the camera. This emissivity parameter is measured in the laboratory by the hemispherical reflectance method. The result is presented versus temperature on Fig. 9.

Before turning on the heating source, we record the measurement noise for a finite duration. The initial time t_0 and the heating duration are marked on the stored thermographic image.

Table 1
Characteristics of the sample

	Density	Calorific capacity	Thickness	Grain diameter	Cell diameter
Glass powder	2500	750	5	0.2–0.25 mm	40 mm
Interstitial fluid(air)	1.16	1007			
Copper	8940	384.9	0.65		

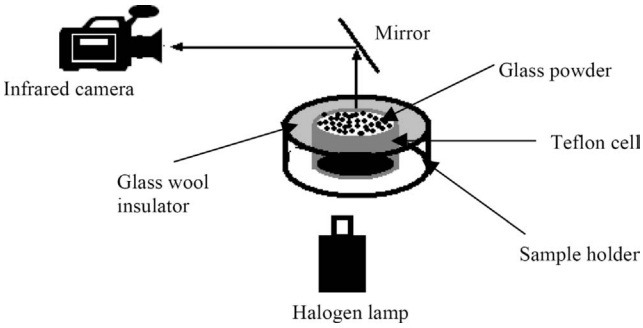

Fig. 7. Experimental device.

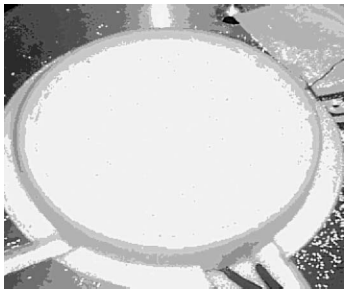

Fig. 8. Glass powder sample.

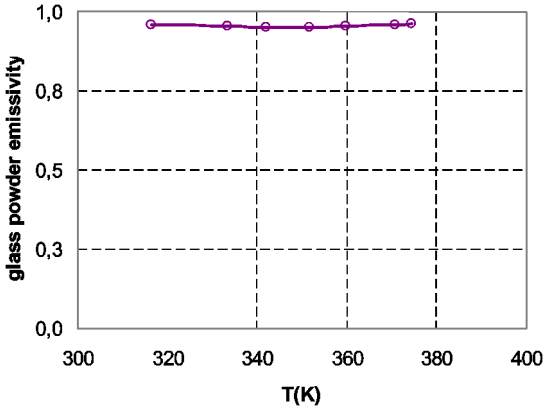

Fig. 9. Emissivity of the glass powder versus temperature.

7. Results and discussion

The measurement of the effective thermal conductivity and the effective thermal diffusivity of the glass powder has been performed in air at room temperature. For evaluation of the thermal parameters, we have used the Gauss–Newton fitting algorithm. The volumetric heat capacity of the powder is calculated using this expression:

$$\rho C_e = \rho C_{p2} = \varepsilon \rho_f C_{pf} + (1-\varepsilon)\rho_s C_{ps} = 1.27 \times 10^6 \ \text{J·K}^{-1}\text{·m}^{-3}$$

The subscripts f and s are relative to fluid (air) and solid (glass grain). Using these values, the parameter β_{r4} is fixed at a known value 0.351. Two experimental estimations are carried out. In the first case, we estimate the four parameters, whereas, in the second case, we impose $\beta_{r5} = 0$ and we

estimate only three parameters. The comparison between the two results shows that the accuracy of the estimated parameters in the second case is higher than this in the first case. In this work, the sample is a glass powder in contact with a copper coating. The thermal contact resistance can be due only to possible flux line constrictions, either in copper, or in the glass grains in contact with its coating. For copper which is a very conducting material, the constriction resistances are negligible. For glass powder, giving that the temperature is measured at the rear face and the medium is supposed to be homogenized, these constriction resistances are incorporated in the equivalent conductivity of the homogenized medium. For these reasons, we choose to neglect the thermal contact resistance and to estimate only three parameters.

The identification procedure converges to final values presented on Table 2. It can be seen that the three parameters are estimated with high accuracy (relative uncertainty does not exceed 2%). The evolutions of the estimated parameters versus experimental duration are presented on Fig. 10. We note that the parameters variation is random for short times and becomes stable for long durations.

Using the definitions given in (Eq. (13)), we can derive the dimensional parameters. The obtained results are given on Table 3. The measured effective thermal conductivity is compared to the calculated value [4] by:

$$k_e^+ = \frac{k_e}{k_f} = \left(\frac{k_s}{k_f}\right)^{0.280-0.757\log(\varepsilon)-0.057\log(k_s/k_f)}$$

where k_s, k_f, k_e and k_e^+ are the solid, fluid thermal conductivity, the effective thermal conductivity and the dimensionless effective thermal conductivity, respectively. The calculated effective thermal conductivity is $k_e = 0.197$

Table 2
Estimated parameters and relative uncertainty

	Estimated values	Standard deviation	Relative uncertainty [%]
$\hat{\beta}_{r1}$	5.38×10^{-3}	1.5190×10^{-5}	0.477
$\hat{\beta}_{r2}$	3.464×10^{-1}	6.88×10^{-3}	1.98
$\hat{\beta}_{r3}$	2.08×10^{-1}	1.366×10^{-3}	0.672

Table 3
Measured dimensional parameters

Parameters	Values	Relative uncertainty [%]
a_e ($m^2 \cdot s^{-1}$)	1.34×10^{-7}	4.47
k_e ($W \cdot m^{-1} \cdot K^{-1}$)	0.172	6.47
h ($W \cdot m^{-2} \cdot K^{-1}$)	11.80	10.45

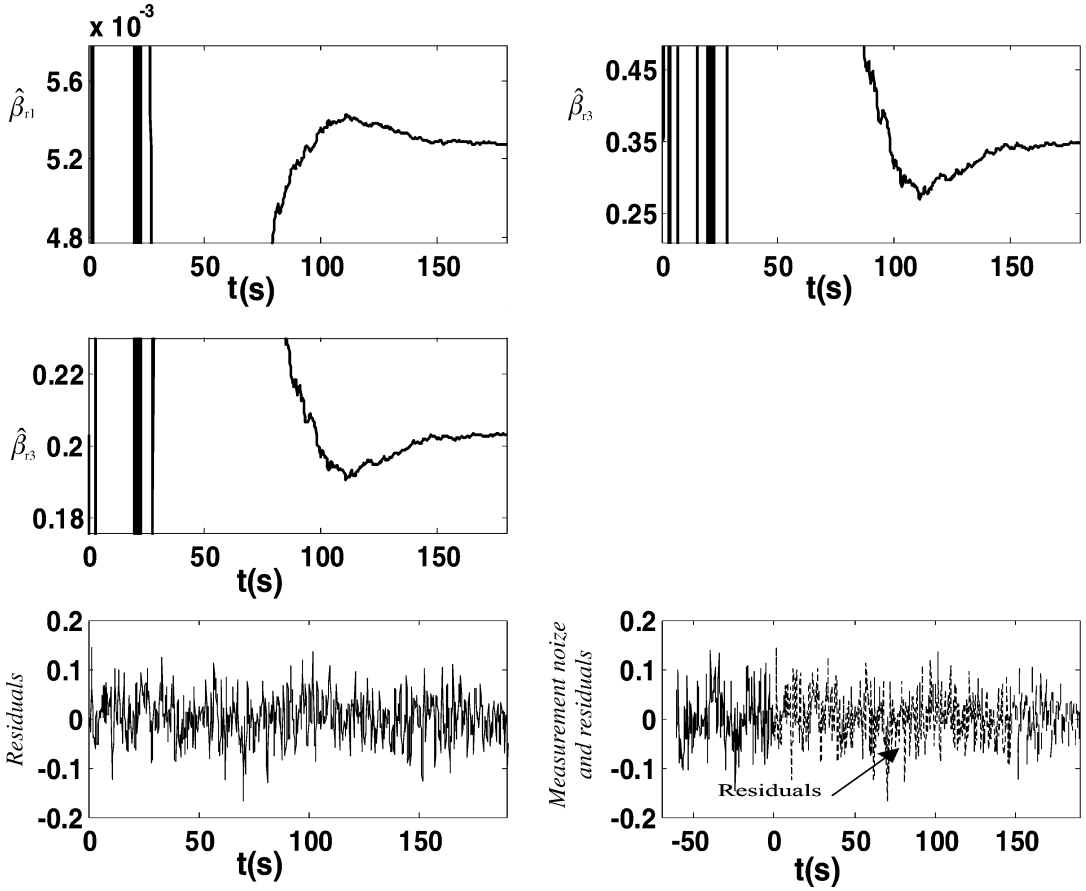

Fig. 10. Variation of the estimated parameters versus experiment duration, Residuals between measured and calculated temperature and comparison between residuals and measurement noise.

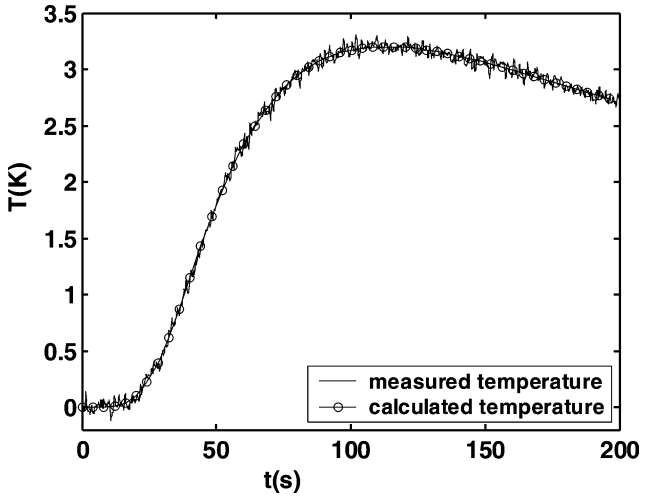

Fig. 11. Comparison between measured and calculated temperature for a glass powder.

$W{\cdot}m^{-1}{\cdot}k^{-1}$, which is close to the measured value $k_e = 0.172\ W{\cdot}m^{-1}{\cdot}k^{-1}$.

The uncertainties on the effective thermal diffusivity and conductivity are calculated using these expressions:

$$\frac{\Delta a_e}{a_e} = \frac{\Delta \beta_{r1}}{\beta_{r1}} + 2\frac{\Delta e_2}{e_2}$$

$$\frac{\Delta k_e}{k_e} = \frac{\Delta a_e}{a_e} + \frac{\Delta \rho C_e}{\rho C_e}$$

The thickness of the substrate and the volumetric heat capacity are known with an accuracy of 2%, the effective thermal diffusivity and the effective thermal conductivity are then calculated with an accuracy of 5% and 7%, respectively. The effective thermal conductivity of this type of glass powder has been experimentally measured and theoretically analyzed with help of the hot wire method [3–5]. The obtained results show a great agreement with our results.

In order to check these results, we calculated the temperature using the estimated parameters. Fig. 11 shows comparisons between the experimental and the calculated temperature. We notice a good agreement between the curves. The residue is compared to the measurement noise and represented on Fig. 10. We remark that the residuals are random and centered on zero.

8. Conclusion

This work has shown that using a crenel heating excitation and the Gauss–Newton parameter estimation procedure, the effective thermal conductivity and the effective thermal diffusivity of a powder can be estimated with a high precision. The thermal model of the rear face temperature is developed and reparameterized in dimensionless form. Analysis of sensitivity coefficients provides information about estimation possibilities for each parameter. An optimality criterion was presented and optimal conditions including heating time and experiment duration were studied. The identification result of the effective thermal conductivity is validated with literature results and the accuracy of the estimated parameter was analyzed.

References

[1] W. Woodside, J.H. Messmer, Thermal conductivity of porous media. I. Unconsolidated sands, J. Appl. Phys. 32 (1961) 1688–1698.
[2] E. Hahne, Y.W. Song, U. Gross, Measurements of the thermal conductivity in porous media, Convect. Heat Mass Transfer Porous Media (1991) 849–865.
[3] P. Dumez, La conductivité thermique des matériaux pulvérulents et granulaires et ses méthodes de mesure en régime établi, Rev. Gen. Ther. 55 (1966) 673–686.
[4] Y. Feng, B. Yu, M. Zou, D. Zhang, A generalized model for the effective thermal conductivity of porous media based on self-similarity, J. Phys. D: Appl. Phys. 37 (2004) 3030–3040.
[5] S. Melka, J.J. Bézian, L'isolation thermique par les matériaux granulaires, Rev. Gen. Ther. 36 (1997) 345–353.
[6] W.J. Parker, R.J. Jenkins, C.P. Buttler, G.L. Abbott, Flash method of determining thermal diffusivity, heat capacity and thermal conductivity, J. Appl. Phys. 32 (1961) 1679–1684.
[7] L. Vozàr, T. Sramkovà, Two data reduction methods for evaluation of thermal diffusivity from step-heating measurements, Internat. J. Heat Mass Transfer 40 (1997) 1647–1655.
[8] K.J. Dowing, B.F. Blackwell, Design of experiments to estimate temperature dependent thermal properties, Inverse Problems Engrg. (1999).
[9] D. Maillet, C. Moyne, B. Rémy, Effect of a thin layer on the measurement of the thermal diffusivity of a material by a flash method, Internat. J. Heat Mass Transfer 43 (2000) 4057–4060.
[10] E.G. Wollf, D.A. Schnieder, Prediction of the thermal contact resistance between polished surfaces, Internat. J. Heat Mass Transfer 41 (1998) 3469–3482.
[11] N.D. Milosevic, M. Raynaud, K.D. Maglic, Estimation of thermal contact resistance between the materials of double-layer sample using the laser flash method, Inverse Problems Engrg. 10 (2002) 85–103.
[12] W. Hohenhauer, L. Vozar, An estimation of thermophysical properties of layered materials by the laser flash method, High Temp. High Press. 33 (2001) 17–25.
[13] J.P. Bardon, Introduction à l'étude des résistances thermiques de contact, Rev. Gen. Ther. (1972) 125–429.
[14] A. Degiovanni, A.S. Lamine, C. Moyne, Thermal contact in transient states: A new model and two experiments, J. Thermophys. Heat Transfer 6 (2) (1992) 356.
[15] P.J. Holliday, R. Parker, R.B. Piggott, A.C. Smith, D.C. Steer, Estimation of the thermal contact resistance between potato granules and steel, J. Food Engrg. 28 (1996) 261–270.
[16] F. Gabriel, J.P. Bardon, D. Guilbard, J.C. Rouffignac, Etude de la résistance thermique de contact entre l'étain en cours de fusion et un creuset refroidi, Rev. Gen. Ther. 36 (1997) 354–370.
[17] C.L. Yeh, Y.F. Chen, C.Y. Wen, K.T. Li, Measurement of the thermal contact resistance of aluminium honey combs, Experimental Thermal Fluid Sci. 27 (2003) 271–281.
[18] D. Maillet, S. André, J.-C. Batsale, A. Degiovanni, C. Moyne, Thermal Quadrupoles, Solving the Heat Equation Through Integral Transforms, Wiley, New York, 2000.
[19] M.N. Ozisik, H.R.B. Orlande, Inverse Heat Transfer, Taylor & Francis, New York, 2000.
[20] R. Taktak, J.V. Beck, E.P. Scott, Optimal experimental design for estimating thermal properties of composite materials, Internat. J. Heat Mass Transfer 36 (1993) 2977–2986.
[21] J.V. Beck, K.J. Arnold, Parameter Estimation in Engineering and Science, Wiley, New York, 1977.